Journal of Catalysis 284 (2011) 102–108

Contents lists available at SciVerse ScienceDirect

Journal of Catalysis

journal homepage: www.elsevier.com/locate/jcat

Catalytic effects of ruthenium particle size on the Fischer–Tropsch Synthesis

Juan María González Carballo [a], Jia Yang [b], Anders Holmen [b], Sergio García-Rodríguez [a], Sergio Rojas [a,*], Manuel Ojeda [a], José Luis G. Fierro [a]

[a] Grupo de Energía y Química Sostenibles (EQS), Instituto de Catálisis y Petroleoquímica, CSIC, C/Marie Curie 2, 28049 Madrid, Spain
[b] Department of Chemical Engineering, Norwegian University of Science and Technology (NTNU), NO-7491, Trondheim, Norway

ARTICLE INFO

Article history:
Received 8 June 2011
Revised 19 August 2011
Accepted 7 September 2011
Available online 7 October 2011

Keywords:
Size effects
Ru
SITTKA
Fischer–Tropsch
Kinetics

ABSTRACT

This work investigates the catalytic consequences of Ru cluster size in the Fischer–Tropsch Synthesis (FTS). Ru/Al_2O_3 catalysts with different metal particles size have been obtained by treating the solid in pure H_2 at increasing temperatures and times. Steady-state isotopic transient kinetic analysis (SSITKA) has been carried out at 523 K, 5.5 kPa CO, 55 kPa H_2, and 124.5 kPa inert in order to determine surface residence times and coverage of reversibly bonded CO and CH_x intermediates as a function of Ru particle size (4–23 nm). We have found that FTS with Ru-based catalysts is a highly structure-sensitive reaction when Ru < 10 nm. In this range, turnover frequency of CO consumption (TOF_{CO}) increases as the particle size increases, reaching a constant value for Ru particles larger than 10 nm. The lower intrinsic activity shown by Ru clusters <10 nm may be related to the stronger CO adsorption and concomitant partial blocking of active sites, as suggested by the decreased CO surface residence time as the Ru cluster size increases in the range below 10 nm.

1. Introduction

The Fischer–Tropsch Synthesis (FTS) is a sensible process to obtain clean liquid fuels (paraffins and olefins) from synthesis gas or syngas, a mixture of H_2 and CO in different proportions depending on the source (typically natural gas or coal) and technology used in its manufacture [1]. The renewed interest in the FTS accounts to the possibility of obtaining liquid fuels from syngas either derived from natural gas (*gas-to-liquids*, GTL) or renewable feedstock such as biomass (*biomass-to-liquids*, BTL) [2]. FTS is considered as a polymerization process in which the reaction monomers are formed *in situ* via unassisted and H-assisted CO dissociation steps [3–5]. Fe- and Co-based materials are the archetypal and the most investigated catalysts for FTS [6–9], although Ru is known as the most active metal for this reaction. Furthermore, higher selectivities to long-chain hydrocarbons can be achieved with Ru-based catalysts and the process can be operated in the presence of H_2O and other oxygenate-containing atmospheres, which is an important requisite to successfully convert biomass-derived syngas to biofuels [1,9–12].

Reactions involving CO dissociation steps are known to be mostly structure-sensitive reactions, that is, rates depend on catalyst particle size; at least, it does within a certain range [5,13]. Contradictory results concerning the effects of Co clusters size on FTS have been reported previously, although a number of recent studies have found that Co size indeed possesses a significant influence on measured rates. Thus, Bezemer et al. [14] investigated Co particles of different size (2.6–27 nm) as catalysts for FTS at low (100 kPa) and high pressure (3.5 MPa) and concluded that turnover frequencies of CO consumption (TOF_{CO}) did not depend on Co particle size when metallic clusters were larger than 6–8 nm. In contrast, normalized rates decreased significantly for smaller Co clusters. Later, steady-state isotopic transient kinetic analysis (SSITKA) was carried out in order to determine surface residence times and coverages of the reaction intermediates, with the aim of clarifying the origin of these Co size effects [15]. A higher surface coverage of irreversibly bonded CO was found for smaller Co particles, which was ascribed to a larger fraction of under-coordinated surface sites. It was proposed that the decrease in normalized rates for small Co clusters was caused by a combination of two effects: blocking of edge/corner sites and a lower intrinsic activity at the terraces. SSITKA analysis has confirmed the presence of very strongly bonded carbon and oxygen surface species on the smaller Co particles that act as site blocking species in FTS reactions [16]. Recently, Prieto et al. [17] have reported optimum FTS activity with zeolite-supported Co clusters of 10 nm; larger clusters (up to 141 nm) do not exhibit different intrinsic activities, while smaller particles are less active because of the formation of partially oxidized Co species ($Co^{\delta+}$) at the Co-support interface.

Analogous and detailed investigations on the catalytic effects of Ru clusters size in FTS are scarce, even though Ru catalysts exhibit the highest reported rates in CO hydrogenation reactions. Some authors have suggested that Ru particle size plays a key role in

* Corresponding author.
E-mail address: srojas@icp.csic.es (S. Rojas).

0021-9517/$ - see front matter © 2011 Elsevier Inc. All rights reserved.
doi:10.1016/j.jcat.2011.09.008

the performance of these catalysts in FTS [12,18,19]. For instance, an optimum size of ~7 nm in terms of both CO hydrogenation rate and heavy hydrocarbons productivity has been reported with Ru clusters deposited on carbon nanotubes [12]. Other reports suggest, however, a lack of relationship between measured reaction rates and Ru clusters size [20,21]. We anticipate that this structure-insensitivity may be related to the fact that these latter investigations have considered a somewhat narrow range of Ru particle sizes.

SSITKA technique has been used in the last years to investigate the effects of alkali promotion, H_2 pressures, and temperature in FTS reactions with supported Ru catalysts [22–24]. Here, we have employed this technique to explore the catalytic effects of Ru particle size in FTS. We show that H_2 + CO turnover frequencies increased with Ru clusters size in the range 4–10 nm, while it remains fairly constant for larger particles (up to 23 nm). The lower intrinsic activity of the small Ru particles (<10 nm) may be related to the strong adsorption of surface species and concomitant blocking of active sites.

2. Experimental

2.1. Catalysts preparation

Ru supported on γ-Al_2O_3 (1.8 wt.% metal loading, 240 $m^2\ g^{-1}$) was prepared by the incipient wetness impregnation method. Ru(NO)$(NO_3)_3$ (31.30%, Alfa Aesar) was dissolved in distilled H_2O and added dropwise to the support. The solid was then dried at room temperature for 12 h and named as Ru/Al_2O_3. Different aliquots (50 mg) were treated under H_2 flow (50 $cm^3\ min^{-1}$) at increasing temperatures (523–973 K) and times (1–3 h) in order to obtain Ru clusters of different size. Catalysts are named here as *x*Ru, where *x* denotes the metallic cluster size (nm) determined from H_2 chemisorption data (see later).

2.2. Physicochemical characterization

Total-reflection X-ray fluorescence (TXRF) was used to determine the exact Ru loading in the fresh Ru/Al_2O_3 solid following experimental protocols previously reported [25].

Temperature-programmed reduction (H_2-TPR) of the fresh sample was carried out in a U-shaped quartz reactor. Prior to the reduction experiment, the sample (15 mg) was flushed with a He stream at 373 K for 30 min and then cooled down to room temperature. The H_2-TPR profile was obtained by heating the sample under a 10% H_2/Ar flow (50 $cm^3\ min^{-1}$) from 303 to 1173 K at a rate of 10 K min^{-1}.

Dispersion and size of the Ru particles were calculated from volumetric H_2 chemisorption data measured on a Micromeritics ASAP 2020 instrument. Experimentally, 150 mg of the fresh sample was loaded in a U-shaped quartz reactor, where it was initially evacuated at 373 K (10 K min^{-1}) for 30 min. Afterward, the sample was treated in 10 $cm^3\ min^{-1}$ pure H_2 at the desired temperature at a heating rate of 10 K min^{-1}, evacuated under vacuum subsequently at the same temperature for 0.5 h, and finally, cooled down to 373 K. H_2 adsorption experiments were performed at 373 K, according to previous reports [26]. Adsorbed H_2 was determined by extrapolation to zero pressure of the linear part of the adsorption isotherm in the interval 0.3–13 kPa and assuming a chemisorption stoichiometry H/Ru = 1 [26].

Micrographs of selected samples were obtained with a JEM-2100F 200 kV transmission electron microscope (JEOL Ltd.) equipped with an Oxford INCAx-Sight EDS detector (Oxford Instruments Ltd.). High-angle annular dark-field scanning transmission electron microscopy (HAADF-STEM) images were obtained upon operating the microscope in scanning mode with an electron probe size of 1 nm, and the signal was recorded with an annular dark-field detector with an inner collection angle of 59 mrad (Z-contrast) and a maximum point resolution of 0.1 nm.

2.3. Steady-state isotopic transient kinetic analysis (SSITKA)

Details of the SSITKA apparatus used in this work are reported elsewhere [27]. Briefly, a quartz microreactor (4 mm inner diameter) was used; the dead volume of the reactor was minimized by filling the voids with quartz wool and a quartz rod (ø = 3 mm). The isotopic switches were monitored with a Balzers QMG 422 quadrupole mass spectrometer (MS), and the catalytic activity was measured on line with a HP5890 gas chromatograph (GC) equipped with a thermal conductivity and flame ionization detectors to determine the concentrations of C_1–C_7 hydrocarbons, CO, H_2, and Ar.

Reactant gas flows and pressures were regulated with Bronkhorst Hi-Tec mass flow controllers (MFC) and pressure controllers (PC). The switching valve is a Valco 2-position air actuator with a digital valve interface, with a valve transit time of 20 ms. ^{12}CO was passed over a carbonyl trap (PbO). The other gases were used without further purification. The following *m*/*z* fragments were recorded with the mass spectrometer: H_2 (2), $^{12}CH_4$ (15), $^{13}CH_4$ (17), ^{12}CO (28), ^{13}CO (29), Ar (40), and Kr (84).

For the SSITKA experiments, *ca.* 50 mg of sieved catalyst (53–90 μm pellet size) was mixed with SiC (200 mg; 53–90 μm pellet size). The sample was pretreated in H_2 flow (10 $cm^3\ min^{-1}$) at different temperatures and times, depending on the particle size desired taking into account the H_2 chemisorption experiments, followed by cooling to 373 K. The feed was then switched to ^{12}CO/Ar mixture (35 $cm^3\ min^{-1}$, 8 kPa CO, 177 kPa inert).

CO chemisorption at 373 K was determined by switching the ^{12}CO/Ar mixture to ^{13}CO/Kr with identical composition and flow rate (this experiment is denoted as S1). Steady state was reached after 3 min. Subsequently, the feed was switched back to the ^{12}CO/Ar mixture, and H_2 (15 $cm^3\ min^{-1}$) was added before recording further experiments. CO chemisorption in the presence of H_2 was determined by switching the feed from H_2/^{12}CO/Ar to H_2/^{13}CO/Kr (50 $cm^3\ min^{-1}$, 5.5 kPa CO, 55 kPa H_2, 124.5 kPa inert) at 373 K (this experiment is denoted as S2) and 523 K (this experiment is denoted as S3). In order to study the catalyst in its most pristine state, the switch from H_2/^{12}CO/Ar to H_2/^{13}CO/Kr was carried out 5 min after the onset of the reaction. CO conversion was maintained below 10%.

2.4. SSITKA data treatment

Assuming a first-order reaction with no readsorption, the apparent rate constant (k) is given by the reciprocal of the average residence time for the active surface intermediates.

$$k = \tau^{-1} = TOF \times \theta^{-1} \quad (1)$$

where τ is the average residence time of the surface intermediates, *TOF* is the turnover frequency, and θ denotes the surface coverage. The average residence time is calculated from the area under the normalized transient curve, $F_i(t)$:

$$\tau_i = \int_0^\infty F_i(t)dt \quad (2)$$

The measured average residence times are corrected for gas phase hold-up by using the inert switching (Ar to Kr).

Due to the delay of product transient as a consequence of the adsorption and desorption of CO on the surface, the average resi-

dence time of the intermediates leading to methane (τ_{CHx}) is corrected taken into account this chromatographic effect for CO [28]:

$$\tau_{CH_x,corr} = \tau_{CH_x,meas} - 0.5\tau_{CO} \quad (3)$$

The number of adsorbed species (N_i) is calculated from the mean residence time and the exit flow (EF) of the species i (i = CH_x, CO):

$$N_i = \tau_i \times EF_{i,exit} \quad (4)$$

Turnover frequencies are calculated based on the number of active sites determined by H_2 chemisorption.

3. Results and discussion

3.1. Catalyst characterization

The Ru content of the fresh Ru/Al_2O_3 solid is 1.8 wt.%, as determined by TXRF. The H_2-TPR profile of the fresh sample (not shown) records a single symmetric peak centered at *ca.* 483 K that suggests a uniform distribution of the Ru particles on the support [29]. Formation of RuO_x–Al_2O_3 mixed oxide phases can be discarded because of the absence of further H_2 consumption features [24]. This is not unexpected because noble metal nanoparticles deposited on γ-Al_2O_3 require higher temperatures and oxidizing atmospheres to form mixed oxides [30]. Based on the temperature of the maximum reduction rate, a slightly higher temperature (523 K) was selected as the lower reduction temperature in order to obtain the different Ru particle sizes during the thermal treatment in H_2 of the fresh sample.

Two techniques were used to establish the Ru mean particle size of the catalysts namely static H_2 chemisorption and STEM. CO chemisorption from SSITKA could be a complementary method for evaluating metal dispersion. However, it has been recently reported that whereas SSITKA is a reliable technique for evaluating Co dispersion, its application for metals such as Ru is limited [31]. Table 1 depicts Ru clusters' sizes determined from H_2 chemisorption data obtained with the Ru/Al_2O_3 solid treated in H_2 at increasing temperatures and times. We have found increased Ru particles with the severity of the thermal treatment [32,33]. Thus, Ru particles of 4 nm were obtained after the thermal treatment in H_2 at 523 K for 1 h, increasing up to 23 nm after the treatment at 923 K for 3 h. No significant changes in Ru cluster size were observed in the 523–773 K range (not shown).

Selected representative STEM images of the Ru/Al_2O_3 catalysts treated at different temperatures along with the particle size distributions are shown in Fig. 1. Ru/Al_2O_3 solid treated at 523 K for 1 h exhibits a homogeneous distribution of Ru particles (2.0 ± 0.3 nm; Fig. 1a). As the severity of the reduction process is increased, the Ru particles tend to sinter yielding oval-shaped Ru agglomerates (Fig. 1b and c). A closer inspection of the micrographs of the sample treated at 923 K (Fig. 1b) shows the presence of non-aggregated small Ru particles of ~1 nm (white circle in Fig. 1b). Consequently, the histogram shows a bi-modal particle size distribution; the smaller particles ~1–2 nm are those that have not sintered during the thermal treatment, whereas the larger particles of ~6 nm account to the sintering of the Ru particles. The longest dimension of the oval-shaped particles was considered for determining particle size. A single average particle size of Ru has been calculated from the bi-modal distribution by using the following equation reported by Borodziński and Bonarowska [34] for a collection of particles of identical shape but of different sizes:

$$d = \frac{\sum_i n_i d_i^3}{\sum_i n_i d_i^2} \quad (5)$$

where n_i is the number of Ru clusters with diameter d_i.

Mean Ru cluster sizes calculated from H_2 chemisorption data and STEM images are compared in Table 1. Results derived from both techniques are in good agreement and reveal that the Ru particle size increases with the severity of the thermal treatment.

3.2. CO chemisorption on Ru determined by SSITKA

Fig. 2 shows the transients corresponding to the CO/inert switch at 373 K (experiment S1) with the 4Ru sample (Ru/Al_2O_3 pretreated in H_2 at 523 K for 1 h). The H_2/CO/inert switch at 373 K (experiment S2) gave a similar transient behavior (not shown). A remarkable difference between the inert transients and the CO transients due to the reversible adsorption of CO on Ru catalysts is observed [27]. Table 2 reports the ratio of the CO adsorbed (calculated from the residence time) during the transient from ^{12}CO to ^{13}CO at 373 K in the absence and in the presence of H_2 (CO_{S1} and CO_{S2}, respectively). This ratio is close to 1, which means that the amount of CO adsorbed on the catalyst surface is similar in both cases, i.e., the amount of adsorbed CO seems not to be influenced by the presence of H_2. This observation implies that the average surface residence time and the surface concentration of reversibly adsorbed CO on Ru remain constant, notwithstanding the H_2 pressure range [24,35]. This strongly suggests that adsorbed CO is likely the most abundant species on Ru surfaces under these conditions, as already demonstrated by rigorous kinetic studies on Fe- and Co-based catalysts [3,4]. This is also consistent with previous reports showing that the enthalpy of CO adsorption ($-\Delta H_{ads}$) on Co and Fe catalysts is higher than that corresponding to H_2 [3,27].

3.3. Fischer–Tropsch Synthesis studies by SSITKA

Fig. 3 shows the transient behavior of the H_2/CO/inert switch (experiment S3) performed after 5 min of time on stream (TOS) with the 4Ru sample. Similar transients were obtained with the catalysts pretreated at increasing temperatures (523–973 K) and times (1–3 h). The calculated residence times of surface CO (τ_{CO}) and CH_x (τ_{CHx}) species for all the Al_2O_3-supported Ru clusters are reported in Table 2. CO residence time increases as Ru particle size decreases in the range 4–10 nm. In contrast with previous studies

Table 1
Thermal treatment protocols and size of Ru clusters determined from H_2 chemisorption data and STEM images.

Sample	H_2 treatment		Dispersion (%)[a]	Cluster size (nm)		Exposed Ru (mmol g_{cat}^{-1})[a]
	Temp. (K)	Time (h)		H_2-chem.	STEM	
4Ru	523	1	32	4	2.0 ± 0.3	0.047
5Ru	773	1	27	5	–	0.040
7Ru	873	1	20	7	–	0.030
8Ru	923	1	16	8	6.0 ± 1.9	0.024
12Ru	973	1	11	12	12.0 ± 4.0	0.016
16Ru	973	2	8	16	–	0.012
23Ru	973	3	6	23	–	0.009

[a] Determined from H_2 chemisorption.

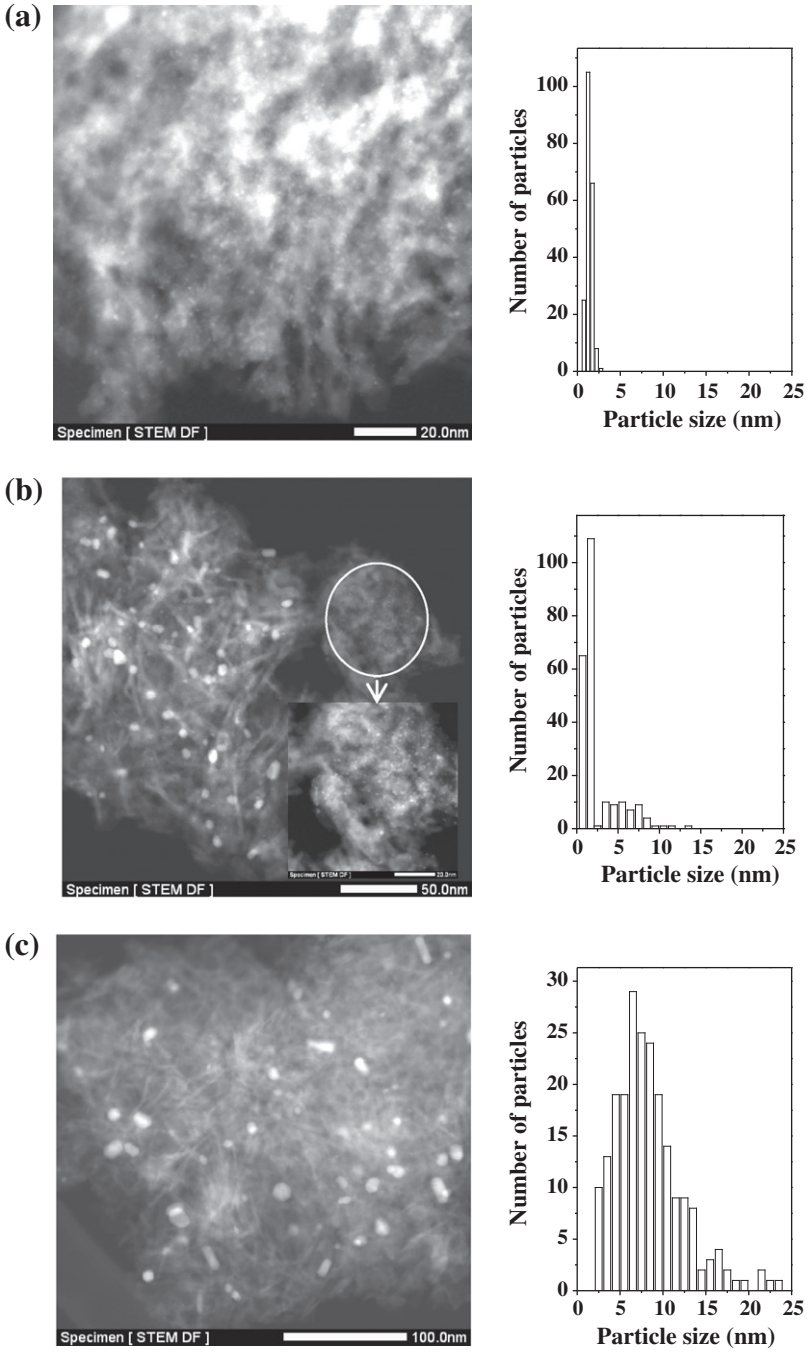

Fig. 1. STEM images and histograms of the samples: 4Ru (a), 8Ru (b), and 12Ru (c). The inset to 8Ru is a magnification of the region with the smaller Ru particles.

on Co clusters of similar size [15], our observation suggests a stronger CO adsorption on the smaller Ru particles. Admittedly, the increasing CO residence time could be also explained by a higher amount of adsorption sites on the smaller particles. On the contrary, the residence time of surface CH_x species seems to be independent on Ru particles size, at least in the range studied here (4–23 nm). A different trend has been reported for Co-based catalysts, for which the residence time of surface CH_x species increases as Co cluster size decreases from 6 nm [15]. Such different performance may account for the higher ability of Ru clusters to catalyze the FTS reaction [1]. Since Ru particles are more active than Co ones, we anticipate that the dependence of τ_{CHx} with Ru cluster size would be observable for Ru clusters smaller than 6 nm.

The ratio of the CO adsorbed during FTS catalysis (experiment S3; 523 K; 5.5 kPa CO, 55 kPa H_2, 124.5 kPa inert) and during CO adsorption at 373 K (experiment S2; 8 kPa CO, 177 kPa inert) is shown in Table 2. Similar values of adsorbed CO in both cases are found, which suggest that adsorption temperature does not have an important impact on CO adsorption, in agreement with literature (Ru/SiO_2, 513–543 K) [24].

The surface coverage of CH_x intermediates was calculated from Eq. (1), and surface residence times are reported in Table 2, assuming a 1:1 ratio of CH_x to the Ru surface atoms [15]. Fig. 4a shows the variation of the CH_x surface coverage with the size of ruthenium particles. The surface coverage of the intermediates decreased for Ru cluster sizes below 10 nm, while the values obtained for Ru par-

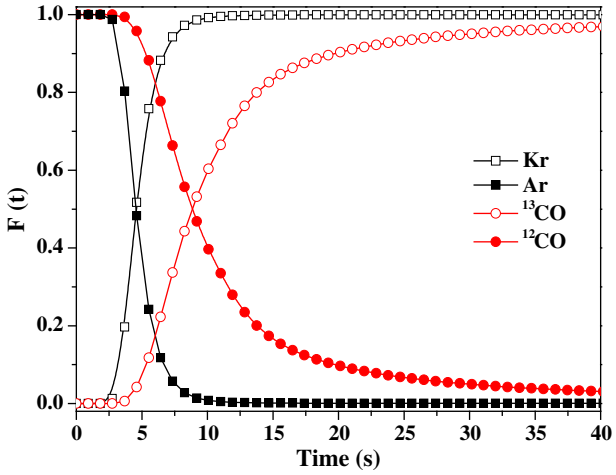

Fig. 2. Transients from ^{12}CO/inert to ^{13}CO/inert switch (373 K; 8 kPa CO, 177 kPa inert) obtained with the catalyst 4Ru (Ru/Al_2O_3 pretreated in H_2 at 523 K for 1 h).

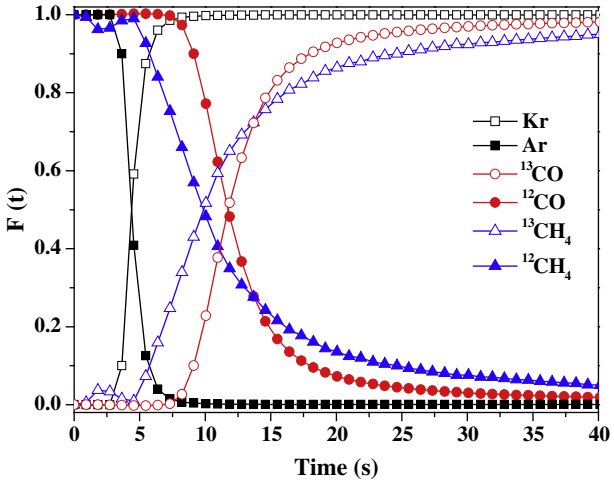

Fig. 3. Transients from $H_2/^{12}CO$/inert to $H_2/^{13}CO$/inert switch (523 K; 5.5 kPa CO, 55 kPa H_2, 124.5 kPa inert) obtained with 4Ru (Ru/Al_2O_3 pretreated in H_2 at 523 K for 1 h).

Table 2
Summary of CO adsorption and average residence time of surface species (CO and CH_x) obtained from SSITKA experiments.

Ru size (nm)[a]	CO_{S1}/CO_{S2}[b]	τ_{CO} (s)[c]	τ_{CHx} (s)[c]	CO_{S1}/CO_{S3}[d]	θ_{CHx}[e]
4	1.0	9.3	5.4	1.2	0.088
5	1.1	8.1	4.8	1.2	0.118
7	0.9	8.3	5.4	1.3	0.194
8	1.2	8.4	5.4	1.3	0.203
12	1.1	7.0	5.0	1.0	0.330
16	1.0	7.1	4.8	1.0	0.340
23	1.1	7.7	5.7	1.0	0.335

[a] Based on H_2 chemisorption.
[b] Ratio of the amount of CO adsorbed at 373 K obtained from the transients S1 and S2 (see Section 2.3). The surface residence times are not shown.
[c] τ_i: residence time of CO and CH_x intermediates obtained at 523 K (transient S3, see Section 2.3).
[d] Ratio of the amount of CO adsorbed during FTS at 523 K (S3) and the CO adsorbed during the transient S1 (see Section 2.3).
[e] θ_{CHx}: surface coverage of CH_x intermediates.

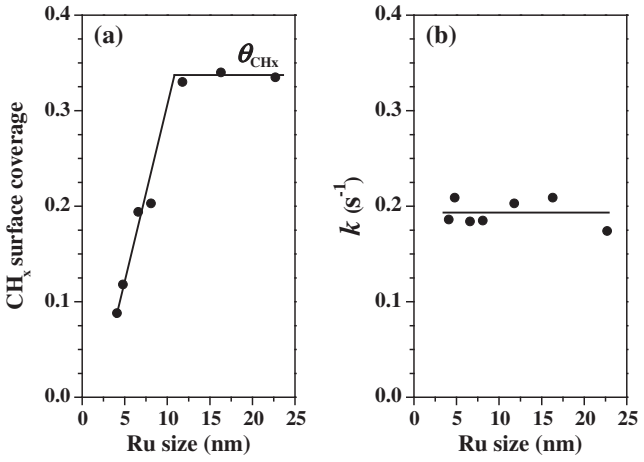

Fig. 4. Effects of Ru cluster size on surface coverage of the reaction intermediates (a) and apparent rate constant (b). Reaction conditions: 523 K; 5.5 kPa CO, 55 kPa H_2, 124.5 kPa inert.

ticles larger than 10 nm remain almost constant. Furthermore, the apparent rate constant (k) of the methanation reaction was calculated as the reciprocal of the surface residence time of CH_x, assuming a first-order irreversible reaction without readsorption [36]. As shown in Fig. 4b, the values of the rate constant do not vary within the range of particle sizes studied, which means that the Ru particle size does not have any effect on the intrinsic site activity [16,35]. Nonetheless, since the surface coverage of reaction intermediates changes with Ru size (see Fig. 4a), so it does measured turnover frequencies.

Fig. 5 shows normalized FTS rates (5–10% CO conversion, 523 K, 5.5 kPa CO, 55 kPa H_2, 124.5 kPa inert) measured with Ru/Al_2O_3 catalysts with different metallic clusters size. Maximum rates are obtained for Ru clusters of ~10 nm. In contrast, products selectivity is not significantly affected by Ru cluster size (4–23 nm, Fig. 6). The high selectivity to methane (C_1) and the relatively low selectivity to C_{3+} hydrocarbons account for the high H_2-to-CO ratio used in our investigations ($H_2/CO = 10$) in order to minimize catalyst deactivation problems by carbon deposition [35]. Bell and co-worker [18] also reported that neither the probability for chain growth nor the olefin-to-paraffin ratio is affected for Ru dispersions below 0.7, and only a minor decrease in the probability of chain growth is observed at dispersions above such value. Although dispersion values and reaction conditions reported in [18] are slightly different than those reported in our manuscript, the observation that prod-

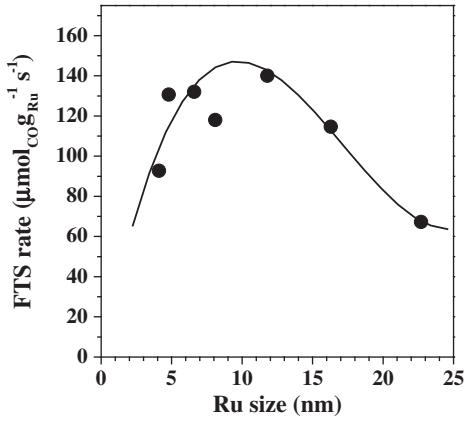

Fig. 5. Normalized FTS rates (5–10% CO conversion, 523 K, 5.5 kPa CO, 55 kPa H_2, 124.5 kPa inert) as a function of Ru particles size.

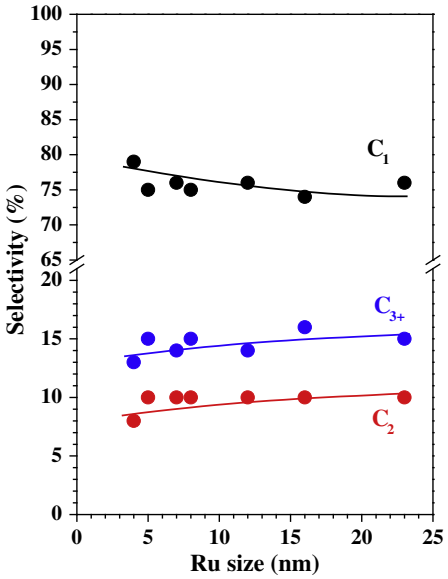

Fig. 6. Effects of Ru cluster size on FTS selectivity. Reaction conditions: 523 K; 5.5 kPa CO, 55 kPa H_2, 124.5 kPa inert.

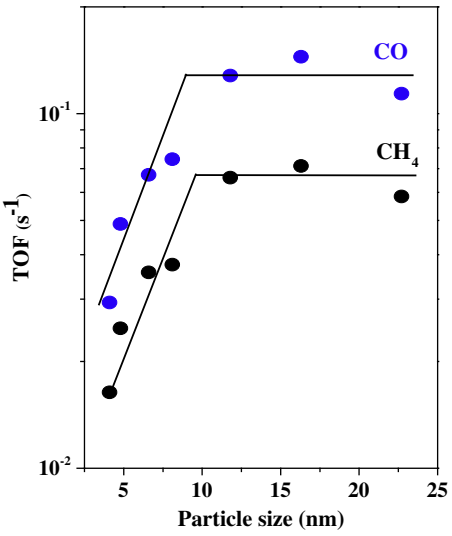

Fig. 7. Effects of Ru cluster size on turnover frequencies for CO consumption and CH_4 formation rates (523 K; 5.5 kPa CO, 55 kPa H_2, 124.5 kPa inert).

Table 3
Turnover frequencies measured for CO consumption (TOF_{CO}) and CH_4 formation (TOF_{CH4}) rates during FTS (523 K; 5.5 kPa CO, 55 kPa H_2, 124.5 kPa inert).

Ru size (nm)	TOF_{CO} (10^{-3} s^{-1})[a]	TOF_{CH4} (10^{-3} s^{-1})[a]
4	29	23
5	49	36
7	67	51
8	74	56
12	129	97
16	145	107
23	114	86

[a] Based on H_2 chemisorption.

uct selectivity is not severely affected by Ru size is common to both works.

Table 3 reports turnover frequencies measured with the Ru catalysts in CO conversion (TOF_{CO}) and CH_4 formation (TOF_{CH4}) rates. Both TOF_{CO} and TOF_{CH4} increase linearly with Ru clusters size for those samples with Ru < 10 nm, but remain essentially unchanged for larger particles (10–23 nm; Fig. 7), that is, FTS on Ru is structure-sensitive when Ru clusters are smaller than 10 nm, but structure-insensitive for larger aggregates. Our results are consistent with a recent report that shows that Ru clusters of about 7 nm lead to optimized FTS catalytic performances in terms of CO consumption rates and productivity to C_{10}–C_{20} hydrocarbons [12]. Kellner and Bell [18] reported that the specific activity for the synthesis of hydrocarbons from CO depended very much on Ru dispersion. Similar Ru sizes (7 nm) have been also found to yield maximum reaction rates in NH_3 decomposition with Ru/γ-Al_2O_3 catalysts [33]. The notion of FTS being a structure-sensitive reaction on Ru, and Co, challenges an early work of Iglesia et al. [21] which reported that the intrinsic activity of Ru surface atoms for the FTS is not influenced by metal dispersion. This discrepancy could account to features such as the effect of the support [37]; it should be remarked that in the work of Iglesia et al. [21], several supports were used, and/or on how the FTS activity is measured; and this work is conducted at conversions <10% (differential reactor conditions), whereas higher CO conversions 45–60% (integral reaction conditions) are reported in [21]. Another important factor to be also taken into account, although a thorough discussion on this topic is out of the scope of this paper, is that the activity of Ru catalysts for the FTS tends to reach similar values after few hours on stream, especially for Ru particles >7 nm when working at high conversion levels (*ca.* 40%). Hence, comparing reaction rates at such conditions could hide the determination of the intrinsic rate of Ru particles.

The number of investigations focused on the effect of Ru size in FTS reactions is very limited. In contrast, these effects have been widely studied for Co-based catalysts [14,15,17]. For instance, Prieto et al. [17] have reported that turnover frequency increases from 0.0012 to 0.0086 s^{-1} (10 wt.% Co/zeolite catalyst, 493 K, 0.6 MPa CO, 1.2 MPa H_2) as the Co particle size increases from 5.6 to 10.4 nm, remaining constant for larger particles. A similar behavior is also found by other authors [15], who have shown that TOF values measured with Co particles (1–22 wt.% Co/carbon nanofibers catalysts, 483 K, 6 kPa CO, 56 kPa H_2) increase in the range 2–6 nm and stay stable hereafter. Recent investigation on model Co catalysts (1.5–7 wt.% Co/SiO_2 catalysts, 513 K, 9.1 kPa CO, 30.3 kPa H_2) has also confirmed increasing turnover frequency values with Co clusters up to 10 nm and stable values for larger aggregates [38]. Similarly, Fe-based catalysts also exhibit enhanced turnover frequencies from 0.06 to 0.187 s^{-1} (5 wt.% Fe/Al_2O_3 catalysts, 573 K, 0.31 MPa CO, 0.63 MPa H_2) as Fe clusters increase from 2 to 6 nm, remaining constant for larger Fe particles [39].

This well-documented cluster size effect on the activity of different reactions has been attributed both to electronic and/or geometrical effects [40]. Thus, Herranz et al. [38] have recently proposed that the decreased ability of small Co clusters to dissociate H_2, evidenced from H_2/D_2 exchange experiments, may well explained their lower FTS turnover frequencies.

Usually, step sites of metallic particles are more reactive than terraces and contribute in a higher extent to measured catalytic activities with metal nanoparticles [41]. Thus, theoretical calculations have proved that N_2 dissociation during NH_3 synthesis with Ru catalysts occurs predominantly (rates about nine orders of magnitude higher) on Ru (0001) steps than on terraces [42], and these higher rates have been attributed to a combination of electronic and geometrical effects. Jacobsen et al. [43] thus concluded that NH_3 synthesis over Ru catalysts is indeed a very structure-sensitive reaction, the activity depending on the size and morphology of the crystals, which are also influenced by the chemical identity of the support material.

Some authors have attributed the stronger CO adsorption on the smaller metal particles as the explanation for their lower catalytic

activity on the CO hydrogenation reaction [15,16]. It has been reported that the highest active site effect is caused by changes in the *d*-band local density of states (LDOS) at the Fermi energy (E_F) at the steps [41]. Since the chemical behavior of transition metal surfaces depends on the *d* state [44,45] and the local reactivity depends on the extent of the backbonding between *d* orbitals and the antibonding CO π^* orbital [46], the larger *d*-LDOS of the smaller particles causes a more pronounced degree of backbonding, hence, the strengthening of the Ru-C bond and the weakening of the C–O bond [47]. The direct consequence of this higher degree of backbonding is the formation of very strongly bonded carbon and oxygen surface species on the smallest particles that blocks the active sites [16]. In this line, den Breejen et al. [15] pointed out to an increased localization of the valence electrons in the surface Co atoms with low coordination number as the reason for the stronger or irreversible CO bonding, whose localization brings about the center of the *d*-band to shift upward and a stronger binding of adsorbates (as CO and carbon and oxygen atoms) to the surface. The decrease in the Fermi energy with decreasing the metal particle size may explain the stronger adsorption of CO and dissociated C and O atoms in the smaller metallic particles.

Here, we have found that the residence time of adsorbed CO (τ_{CO}) increases as the Ru size decreases (<10 nm), which suggests that either smaller particles exhibit more surface vacancies or Ru–CO bond is stronger on such small particles. The former hypothesis would imply that smaller particles should be more active for the FTS. We have observed, however, the opposite trend, and both reaction rate and the TOF for the FTS of the Ru particles decrease as the Ru size goes below 10 nm. Altogether, these observations indicate the formation of stronger Ru–CO bonds in smaller Ru clusters. This line of reasoning is in good agreement with the observation of higher amounts of irreversible adsorbed CO on small Co particles [15]. The lower TOF value shown by these small Ru particles (<10 nm) may be then related to the strong adsorption of CO intermediates and concomitant blocking of active sites, which leads to lower measured turnover frequencies in the FTS reaction. This result is also consistent with a recent theoretical study of the initial step on the FTS on Ru surfaces, which concludes on the one hand that a higher coverage of CO will increase CO activation barrier and that as the particle size decreases the activity for the formation of hydrocarbons is less [5]. Moreover, this explanation is consistent with the absence of Ru cluster size effects on products selectivity. These Ru size effects on H_2/CO reactions are analogous to those already reported for Fe- and Co-based catalysts, and this work provides a general overview of the size effects in FTS catalysis, irrespective of the identity of the metal used as catalyst.

4. Conclusions

We have found that FTS (523 K, 5.5 kPa CO, 55 kPa H_2, and 124.5 kPa inert) with Ru-based catalysts is a highly structure-sensitive reaction when Ru < 10 nm. In this range, turnover frequency of CO consumption (TOF_{CO}) increases as the particle size increases, reaching a constant value for Ru particles larger than 10 nm. The lower TOF shown by Ru clusters <10 nm may be related to the stronger CO adsorption and concomitant partial blocking of active sites, as suggested by the decreased CO surface residence time as the Ru cluster size increases in the range below 10 nm.

Acknowledgments

The authors acknowledge *Ministerio de Educación y Ciencia* (HIREUS ENE2007-67533-C02-02/ALT) and *Comunidad de Madrid* (S2009ENE-1743) for financial support. J.M. González-Carballo also acknowledges *Ministerio de Ciencia e Innovación* and the *Formación de Profesorado Universitario program* (*FPU*) for the Ph.D. grant. M. Ojeda is grateful to the Spanish National Research Council (CSIC) for financial support (JAE-Doc contract).

References

[1] C.N. Hamelink, A.P.C. Faaij, H. den Uil, Energy 29 (2004) 1743.
[2] K. Okabe, K. Murata, M. Nakanishi, T. Ogi, M. Nurunnabi, Y. Liu, Catal. Lett. 128 (2009) 171.
[3] M. Ojeda, R. Nabar, A.U. Nilekar, A. Ishikawa, M. Mavrikakis, E. Iglesia, J. Catal. 272 (2010) 287.
[4] M. Ojeda, A. Li, R. Nabar, A.U. Nilekar, M. Mavrikakis, E. Iglesia, J. Phys. Chem. C 114 (2010) 19761.
[5] S. Shetty, R.A. van Santen, Catal. Today 171 (2011) 168.
[6] M. Ojeda, F.J. Pérez-Alonso, P. Terreros, S. Rojas, T. Herranz, M. López Granados, J.L.G. Fierro, Langmuir 22 (2006) 3131.
[7] F.J. Pérez-Alonso, T. Herranz, S. Rojas, M. Ojeda, M. López Granados, J.L.G. Fierro, J.R. Gancedo, Green Chem. 9 (2007) 663.
[8] A.Y. Khodakov, W. Chu, P. Fongarland, Chem. Rev. 107 (2007) 1692.
[9] G.P. van der Laan, A.A.C.M. Beenackers, Catal. Rev. Sci. Eng. 41 (1999) 255.
[10] M. Claeys, M. van Steen, Catal. Today 71 (2002) 419.
[11] J.P. Hindermann, G.J. Hutchings, A. Kiennemann, Catal. Rev. Sci. Eng. 35 (1993) 1.
[12] J. Kang, S. Zhang, Q. Zhang, Y. Wang, Ang. Chem. Int. Ed. 48 (2009) 2565.
[13] R.A. van Santen, Acc. Chem. Res. 42 (2008) 57.
[14] G.L. Bezemer, J.H. Bitter, H.P.C.E. Kuipers, H. Oosterbeek, J.E. Holewijn, X. Xu, F. Kapteijn, A.J. van Dillen, K.P. de Jong, J. Am. Chem. Soc. 128 (2006) 3956.
[15] J.P. den Breejen, P.B. Radstake, G.L. Bezemer, J.H. Bitter, V. Frøseth, A. Holmen, K.P. de Jong, J. Am. Chem. Soc. 131 (2009) 7197.
[16] J. Yang, E.Z. Tveten, D. Chen, A. Holmen, Langmuir 26 (2010) 16558.
[17] G. Prieto, A. Martínez, P. Concepción, R. Moreno-Tost, J. Catal. 266 (2009) 129.
[18] C.S. Kellner, A.T. Bell, J. Catal. 75 (1982) 251.
[19] K.J. Smith, R.C. Everson, J. Catal. 99 (1986) 349.
[20] R.A. Dalla Betta, A.G. Piken, M. Shelef, J. Catal. 35 (1974) 54.
[21] E. Iglesia, S.L. Soled, R.A. Fiato, J. Catal. 137 (1992) 212.
[22] B. Chen, J.G. Goodwin Jr., J. Catal. 158 (1996) 228.
[23] T.E. Hoost, J.G. Goodwin Jr., J. Catal. 137 (1992) 22.
[24] I.G. Bajusz, J.G. Goodwin Jr., J. Catal. 169 (1997) 157.
[25] R. Fernandez-Ruiz, P. Ocon, M. Montiel, J. Anal. Atom. Spect. 24 (2009) 785.
[26] J. Okal, M. Zawadzki, L. Kepinski, L. Krajczyk, W. Tylus, Appl. Catal. A 319 (2007) 202.
[27] V. Frøseth, S. Storsæter, Ø. Borg, E.A. Blekkan, M. Rønning, A. Holmen, Appl. Catal. A 289 (2005) 10.
[28] C.J. Bertole, C.A. Mims, G. Kiss, J. Catal. 221 (2004) 191.
[29] L. Li, L. Qu, J. Cheng, J. Li, Z. Hao, Appl. Catal. B 88 (2009) 224.
[30] M. Ojeda, S. Rojas, F.J. García-García, M. López Granados, P. Terreros, J.L.G. Fierro, Catal. Commun. 5 (2004) 703.
[31] Y.-T. Tsai, J.G. Goodwin, J. Catal. 281 (2011) 128.
[32] P. Betancourt, A. Rives, R. Hubaut, C.E. Scott, J. Goldwasser, Appl. Catal. A 170 (1998) 307.
[33] A.M. Karim, V. Prasad, G. Mpourmpakis, W.W. Lonergan, A.I. Frenkel, J.G. Chen, D.G. Vlachos, J. Am. Chem. Soc. 131 (2009) 12230.
[34] A. Borodziński, M. Bonarowska, Langmuir 13 (1997) 5613.
[35] J. Panpranot, J.G. Goodwin Jr., A. Sayari, J. Catal. 213 (2003) 78.
[36] S.L. Shannon, J.G. Goodwin Jr., Chem. Rev. 95 (1995) 677.
[37] J.M. Gonzalez Carballo, E. Finocchio, S. Garcia, S. Rojas, M. Ojeda, G. Busca, J.L.G. Fierro, Catal. Sci. Tech. 1 (2011) 1013.
[38] T. Herranz, X. Deng, A. Cabot, J. Guo, M. Salmeron, J. Phys. Chem. B 113 (2009) 10721.
[39] J.Y. Park, Y.J. Lee, P.K. Khanna, K.W. Jun, J.W. Bae, Y.H. Kim, J. Mol. Catal. A: Chem. 323 (2010) 84.
[40] M. Che, C.O. Bennett, The influence of particle size on the catalytic properties of supported metals, in: H.P.D.D. Eley, B.W. Paul (Eds.), Advances in Catalysis, Academic Press, 1989, pp. 55–172.
[41] T. Zambelli, J. Wintterlin, J. Trost, G. Ertl, Science 273 (1996) 1688.
[42] S. Dahl, A. Logadottir, R.C. Egeberg, J.H. Larsen, I. Chorkendorff, E. Törnqvist, J.K. Norskov, Phys. Rev. Lett. 83 (1999) 1814.
[43] C.J.H. Jacobsen, S. Dahl, P.L. Hansen, E. Törnqvist, L. Jensen, H. Topsøe, D.V. Prip, P.B. Møenshaug, I. Chorkendorff, J. Mol. Catal. A: Chem. 163 (2000) 19.
[44] B. Hammer, J.K. Nørskov, Surf. Sci. 343 (1995) 211.
[45] R. Hoffmann, Rev. Mod. Phys. 60 (1988) 601.
[46] H.P. Bonzel, Surf. Sci. Rep. 8 (1988) 43.
[47] P.J. Feibelman, D.R. Hamann, Surf. Sci. 149 (1985) 48.